

Articles

Effects of Ag and Ni Additives on Zn Diffusion in Steel Hot-Dip Galvanizing: An *ab Initio* Molecular Dynamics Simulation

Weihua Zhu, Ping Wu,* Hong Mei Jin, and Hong Lin Liu

Institute of High Performance Computing, 1 Science Park Road, #01-01 The Capricorn, Singapore Science Park II, Singapore 117528, Singapore

Received July 13, 2004. Revised Manuscript Received October 6, 2004

An *ab initio* molecular dynamics study has been performed to investigate the effects of Ag and Ni additives on Zn diffusion in steel hot-dip galvanizing. Ag–Zn, Ni–Zn, and Zn–Zn ensembles are selected to model the industry process. For the Zn–Zn ensemble, the calculated pair correlation function, first peak position, and coordination number are in good agreement with available experimental data. We examine differences in the structural and electronic properties among Ag–Zn, Ni–Zn, and Zn–Zn ensembles. For Zn self-diffusion, we obtain a diffusion constant of 2.48×10^{-9} m²/s, very close to the experimental value of 2.37×10^{-9} m²/s. The Zn diffusion constants of different ensembles increase in the following order: Ag–Zn \approx Zn–Zn > Ni–Zn, which is in agreement with the additive effects on the thickness of coatings in galvanizing, where Ag increases the coating thickness, but Ni decreases it. Our molecular dynamics simulations reveal that the role of additives in controlling the zinc coating thickness is to alter zinc diffusion speed before reaching the substrate. These suggestions may be useful for screening chemical additives to control the zinc coating thickness.

1. Introduction

The generation of zinc coatings on steel is one of the most important processing techniques used to protect steel components exposed to corrosive environments. The zinc coating is composed of a series of Fe–Zn intermetallics and a layer of almost pure zinc. Typical processing methods used in producing zinc coatings include hot-dip galvanizing, thermal spraying, and electrodeposition. Recently, a considerable amount of research has occurred on the hot-dip galvanizing process and on new types of zinc coatings because of new applications in the automotive and building industries.¹ The thickness of the galvanized coatings is a key factor affecting the engineering quality of the coated materials. To control the coating thickness, a proven technique is to incorporate chemical additives in the molten zinc bath. A number of observations^{2–4} indicating the effectiveness of the additives in controlling the coating thickness were accumulated. In our previous studies,^{5,6} we have established the correlation among the additive

behavior, element properties, and crystal structures of binary additive–zinc compounds and predicted many candidates as effective additives. Our density functional theory (DFT) calculations on six types of M–Zn associates (M = Ni, V, Ti, Ag, Sn, and Mg) have shown that the additive effects are attributed to the strong interaction between M and Zn and the charge shift from Zn to M.⁷ To verify the proposed mechanisms in a large number of additives, we used a more realistic cluster model to study all experimentally known additives.⁸ It is found that the interactions between Zn and M are depicted by two structural properties: binding energy and the chemical shift of the Zn 2*p* electronic energy. These structural properties are also correlated with the zinc diffusion coefficients in the presence of the additives. However, as the precise nature of the additive effects is not very clear, there is a pressing need to gain an understanding of Zn diffusion in the presence of the additives at the atomic level.

Diffusion properties are difficult to determine experimentally. Typical experiments to measure diffusion properties are based on tracer diffusion through capillary tubes.⁹ Such experiments suffer from uncertainties arising from the contributions of convection and gravity.

* To whom correspondence should be addressed. Telephone: 65-6419212. Fax: 65-67780522. E-mail: wuping@ihpc.a-star.edu.sg.

(1) Marder, A. R. *Prog. Mater. Sci.* **2000**, *45*, 191.
(2) Mackowiak, J.; Short, N. R. *Int. Met. Rev.* **1979**, *24*, 1.
(3) Rådeker, W.; Friche, W. In *Proceedings of the 7th International Conference on Hot Dip Galvanizing Interlaken*; Pergamon Press: Paris, 1964.
(4) Chen, Z. W.; Kennon, N. F.; See, J. B.; Barter, M. A. *JOM* **1992**, *44*, 22.
(5) Jin, H. M.; Li, Y.; Wu, P. *J. Mater. Res.* **1999**, *15*, 1791.
(6) Wu, P.; Jin, H. M.; Li, Y. *Chem. Mater.* **1999**, *11*, 3166.

(7) Jin, H. M.; Li, Y.; Liu, H. L.; Wu, P. *Chem. Mater.* **2000**, *12*, 1879.

(8) Wu, P.; Jin, H. M.; Liu, H. L. *Chem. Mater.* **2002**, *14*, 832.

(9) Shimoji, M.; Itami, T. A. *Atomic Transport in Liquid Metals*; Trans-Tech Publications: Lancaster, PA, 1986.

These uncertainties can be overcome in principle by carrying out the experiments in microgravity. Another alternative approach is computer simulation. Over the past few years, ab initio molecular dynamics (MD) has become a popular tool for the investigation of materials. In ab initio simulation, the electronic structure is evaluated using DFT and the corresponding forces are used to move the ions according to classical molecular dynamics. This approach can calculate both the atomic and electronic structure consistently and explore how changes in one are correlated with changes in the other. So far ab initio MD has been used to study the dynamic properties of a variety of liquid metals and alloys.^{10–19}

In this paper, we perform ab initio MD simulations to study the effects of the additives Ag and Ni on Zn diffusion in steel hot-dip galvanizing. It is of interest to compare the structures of Ag–Zn and Ni–Zn associates with the structure for the corresponding pure zinc, Zn–Zn, associate. We examine differences in the structural and electronic properties among Ag–Zn, Ni–Zn, and Zn–Zn associates. Diffusion constants of Zn atoms for the dynamic properties of these associates are presented. We discuss the effects of the additives Ag and Ni on the Zn diffusion speed in the molten zinc bath.

The remainder of this paper is organized as follows. A brief description of our computational method is given in section 2. The results and discussion are presented in section 3, followed by a summary of our conclusions in section 4.

2. Computational Method

2.1. Simulation Details. The principles of ab initio MD method have been documented in the literature^{20–24} and will not be reproduced here. Our MD simulations within the framework of DFT were done using the Vienna ab initio simulation package VASP.^{25–28} The package uses a plane-wave expansion of the valence states and a description of the ion–electron interaction in terms of fully nonlocal optimized ultrasoft pseudopotentials similar to those introduced by Vanderbilt.^{29,30} These pseudopotentials allow a smaller basis set for a given accuracy. The residual minimization technique^{27,28} is used to calculate the electronic ground state. The generalized gradient approximation (GGA) proposed by Perdew and Wang,^{31,32} named PW91, was employed, because the

results for the crystalline compounds have been improved by GGA. Ab initio MD simulations were carried out at temperature $T = 723$ K, just above the melting point of pure zinc ($T = 697$ K). We controlled the ionic temperature using a Nosé-thermostat.³³ The equations of motion in the extended phase-space of Nosé-dynamics were integrated by using a Verlet algorithm with a time-step of $\Delta t = 3$ fs. Each ensemble was equilibrated for 3 ps, following which simulations were performed for 6 ps. We used a cutoff of 200 eV for the energies of the plane waves included in the wave function expansion. Brillouin-zone integrations were performed using a grid of Monkhorst–Pack special points.³⁴ We carefully checked convergence with respect to the number of k -points. In the ab initio MD simulations, only the Γ -point was used. The final electronic density of states was recalculated on a larger energy cutoff and a finer k -point mesh for a series of representative configurations.

2.2. Computational Model. The galvanized structure produced in steel hot-dip galvanizing process is usually made of Zn–Fe intermetallic alloy layers, which are composed of zeta, delta, gamma₁, and gamma phases.¹ The outermost phase of zinc coatings is the zeta (ζ) phase, FeZn₁₃. Experimental investigation⁴ shows that an additive of nickel-rich area appeared between the FeZn₁₃ phase and the η phase (a pure zinc phase or the former melting zinc layer). This observation suggests that it may be reasonable to assume the distribution of minor additives is mostly at the interface between molten zinc and the FeZn₁₃ phase. Therefore we may design a supercell with FeZn₁₃ symmetry³⁵ to model additive–zinc compound. A periodical boundary condition was employed in the simulations, and the lattice parameters were adjusted to fit the experimental density of zinc (6.577 g/cm³) at the melting point. For the Zn–Zn ensemble, the unit cell contains 28 zinc atoms. For the additive–zinc ensemble, 2 iron atoms of FeZn₁₃ were substituted by additive element so that the ratio of additive and zinc is the same as the ratio of iron and zinc in the FeZn₁₃ phase. Here we select three systems (Ag–Zn, Ni–Zn, and Zn–Zn) to model the industry process. Among these systems, Zn–Zn represents an industry process without additives, while Ag–Zn and Ni–Zn represent the processes with different additives, since the additives Ag and Ni have opposite effects on the coating thickness. It is experimentally reported that the content of an additive such as nickel is up to 0.1 wt %. To model the system, the model ensemble should contain at least 1000 atoms. At present, this exceeds the capacity of ab initio MD. Since the effects of additives on the zinc diffusion are not very large, and ab initio MD is updated interatomic potential at every simulation step by DFT calculations, a relatively small system size may thus be a compromise between computation efficiency and accuracy. Convergence tests to probe ensemble size are provided in the next section.

3. Results and Discussion

3.1. Tests for Ensemble Size. Ensemble size is a central aspect of ab initio MD simulation. If ensemble size is too small, the simulation can hardly catch the right physics; on the other hand, if ensemble size is very large, the simulation is beyond the capacity of ab initio MD. To balance two requirements, we carried out several tests on different sizes of Zn–Zn ensemble. The direct way to determine ensemble size is through comparing our simulations with experimentally measured structure properties.

Figure 1 gives the pair correlation functions $g(r)$ for different sizes of Zn–Zn ensembles at $T = 723$ K. The

- (10) Kresse, G.; Hafner, J. *Phys. Rev. B* **1994**, *49*, 14251.
 (11) Holender, J. M.; Gillan, M. J.; Payne, M. C.; Simpson, A. *Phys. Rev. B* **1995**, *52*, 967.
 (12) Kresse, G. *J. Non-Cryst. Solids* **1995**, *192&193*, 222.
 (13) Kirchhoff, F.; Holender, J. M.; Gillan, M. J. *Phys. Rev. B* **1996**, *54*, 190.
 (14) Kulkarni, R. V.; Aulbur, W. G.; Stroud, D. *Phys. Rev. B* **1997**, *55*, 6896.
 (15) Kulkarni, R. V.; Stroud, D. *Phys. Rev. B* **1998**, *57*, 10476.
 (16) Costa, B. J.; Martins, J. L. *J. Chem. Phys.* **1999**, *111*, 5067.
 (17) Kulkarni, R. V.; Stroud, D. *Phys. Rev. B* **2000**, *62*, 4991.
 (18) Jain, M.; Godlevsky, V. V.; Derby, J. J.; Chelikowsky, J. R. *Phys. Rev. B* **2001**, *65*, 035212.
 (19) Ko, E.; Jain, M.; Chelikowsky, J. R. *J. Chem. Phys.* **2002**, *117*, 3476.
 (20) Car, R.; Parrinello, M. *Phys. Rev. Lett.* **1985**, *55*, 2471.
 (21) Remler, D. K.; Madden, P. A. *Mol. Phys.* **1990**, *70*, 921.
 (22) Payne, M. C.; Teter, M. P.; Allan, D. C.; Arias, T. A.; Joannopoulos, J. D. *Rev. Mod. Phys.* **1992**, *64*, 1045.
 (23) Tuckerman, M. E.; Ungar, P. J.; von Roseninge, T.; Klein, M. L. *J. Phys. Chem.* **1996**, *100*, 12878.
 (24) Parrinello, M. *Solid State Commun.* **1997**, *102*, 107.
 (25) Kresse, G.; Hafner, J. *Phys. Rev. B* **1993**, *47*, 558.
 (26) Kresse, G.; Hafner, J. *Phys. Rev. B* **1994**, *49*, 14251.
 (27) Kresse, G.; Furthmüller, J. *Comput. Mater. Sci.* **1996**, *6*, 15.
 (28) Kresse, G.; Furthmüller, J. *Phys. Rev. B* **1996**, *54*, 11169.
 (29) Vanderbilt, D. *Phys. Rev. B* **1990**, *41*, 7892.
 (30) Kresse, G.; Hafner, J. *J. Phys. Condens. Matter* **1994**, *6*, 8245.

- (31) Perdew, J. P.; Wang, Y. *Phys. Rev. B* **1992**, *45*, 13244.
 (32) Perdew, J. P.; Chevary, J. A.; Vosko, S. H.; Jackson, K. A.; Pederson, M. R.; Singh, D. J.; Fiolhais, C. *Phys. Rev. B* **1992**, *46*, 6671.
 (33) Nosé, S. *J. Chem. Phys.* **1984**, *81*, 511.
 (34) Monkhorst, H. J.; Pack, J. D. *Phys. Rev. B* **1976**, *13*, 5188.
 (35) Brown, B. P. *Acta Crystallogr.* **1962**, *15*, 608.

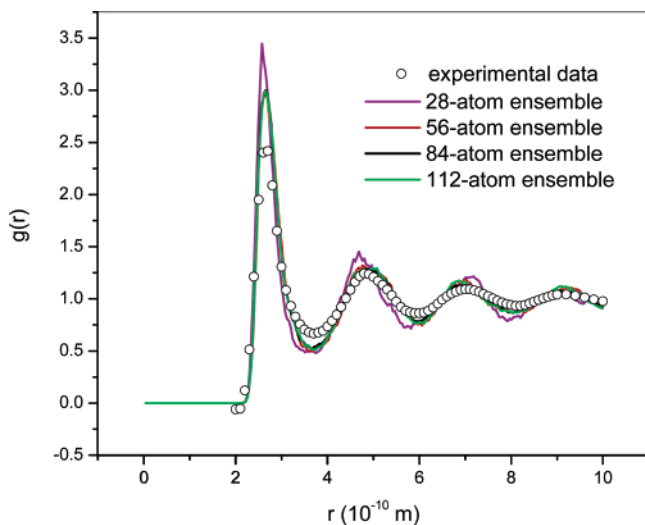


Figure 1. Comparison of the calculated pair correlation functions $g(r)$ for different sizes of Zn–Zn ensemble at 723 K with the experimental results.

experimental results for pure liquid zinc are also listed for comparison. With increasing ensemble sizes, the differences between the calculated and experimental³⁶ $g(r)$ values get smaller and smaller. Moreover, there is no indication of significant differences between the 56-atom, 84-atom, and 112-atom ensembles. It may be seen that the calculated $g(r)$ for the 84-atom ensemble is generally in good agreement with experimental data. We thus use an 84-atom ensemble in all subsequent calculations.

3.2. Structural Properties. The pair correlation function or total radial distribution function $g(r)$ is the probability of finding another atom at a distance r from a specific atom. The information given by $g(r)$ is only one-dimensional, but it does give quantitative information on noncrystalline systems. Therefore, the pair correlation function is one of the most important pieces of information in the study of noncrystalline materials and is frequently employed to examine the structural properties. In Figure 2, we present pair correlation functions $g(r)$ for Ag–Zn, Ni–Zn, and Zn–Zn ensembles at a temperature of 723 K. These are calculated by averaging the positions of zinc atoms for the last 6 ps of our simulations. The evolution patterns of curves for the Ag–Zn, Ni–Zn, and Zn–Zn ensembles show striking similarity. The second, third, and fourth peaks are already substantially damped, compared with the first peak. Overall, it is found that the pair correlation functions have weak long-range correlation in the liquid. We notice that the additions of Ag or Ni do not change the positions of the peaks in the pair correlation function, which remain almost the same as those found for pure liquid zinc, but they alter the maxima and minima of the peaks. The additions of Ag or Ni increase the height of the peaks compared with the pure zinc case.

Coordination number gives a convenient picture of nearest-neighbor atoms in the liquid structure. Hence the coordination number, particularly the first coordination number, is frequently used in the structural study of noncrystalline materials. Given the pair correlation

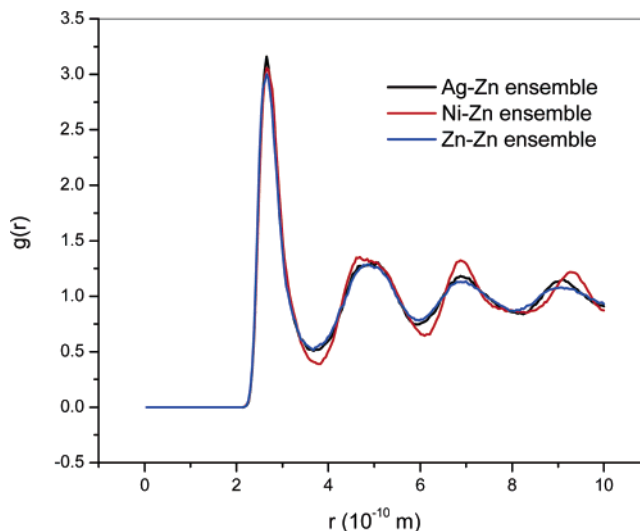


Figure 2. Calculated pair correlation functions $g(r)$ for Ag–Zn, Ni–Zn, and Zn–Zn ensembles at 723 K.

Table 1. Calculated and Measured First Peak Position (Å) and Coordination Number for Ag–Zn, Ni–Zn, and Zn–Zn Ensembles at 723 K

	this work			experiment ^a
	Ag–Zn	Ni–Zn	Zn–Zn	Zn–Zn
first peak position	2.66	2.66	2.66	2.68
coordination number	10.90	11.35	10.87	10.5

^a Ref 36.

functions, it is possible to estimate coordination numbers by integrating $n \times 4\pi r^2 g(r)$ from $r = 0$ to the first minimum r_m after the first peak in $g(r)$, where n is the number density. From the pair correlation functions, we determined the first minimum r_m from $g(r)$ and used them to calculate the coordination numbers. Table 1 gives first peak positions and coordination numbers for the Ag–Zn, Ni–Zn, and Zn–Zn ensembles at 723 K. It can be seen that the principal peak positions of all three pair correlation functions occur at about the same separation, namely 2.66 Å. The coordination number for Zn–Zn ensemble at 723 K is 10.87, in good agreement with the experimental estimate of 10.5.³⁶ The coordination numbers of different ensembles increase in the following order: Ni–Zn > Ag–Zn \approx Zn–Zn. We notice that these values are very close to the value expected in a close-packed liquid, which would be in the range of 9 or 10.

It is interesting to note that the coordination numbers estimated here agree well with the former observations. Our previous study⁶ pointed out that most additive–zinc compounds have a structural type with 12 coordination number. DFT calculations on the relative stability of four possible configurations including MZn_4 , MZn_6 , MZn_8 , and MZn_{12} (M is the additive element)⁷ indicated that the icosahedral MZn_{12} configuration is most stable among these zinc-additives. The reliability of our previous studies is further verified by the ab initio MD simulations considered here.

3.3. Electronic Properties. In this section, we examine the electronic structures of the ensembles. The electronic density of states (DOS) was calculated as the average of a few hundred configurations distributed over the whole simulation. We used a grid of Monkhorst–Pack special points in a small Brillouin-zone corre-

(36) Waseda, Y. *The Structure of Non-Crystalline Materials*; McGraw-Hill Inc: New York, 1980.

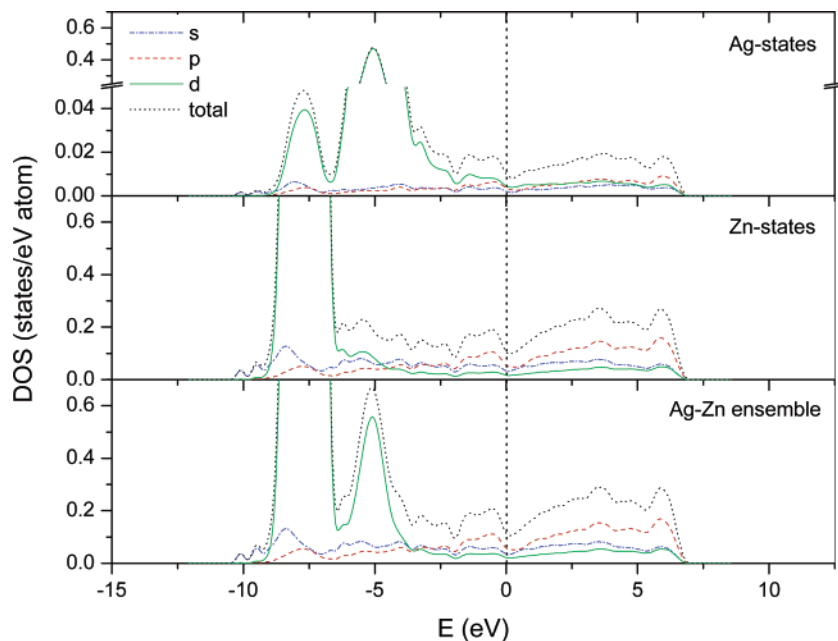


Figure 3. Total and partial density of states (DOS) of Ag-states, Zn-states, and Ag–Zn ensemble averaged over a few hundred configurations. The Fermi energy is shown as a dashed vertical line.

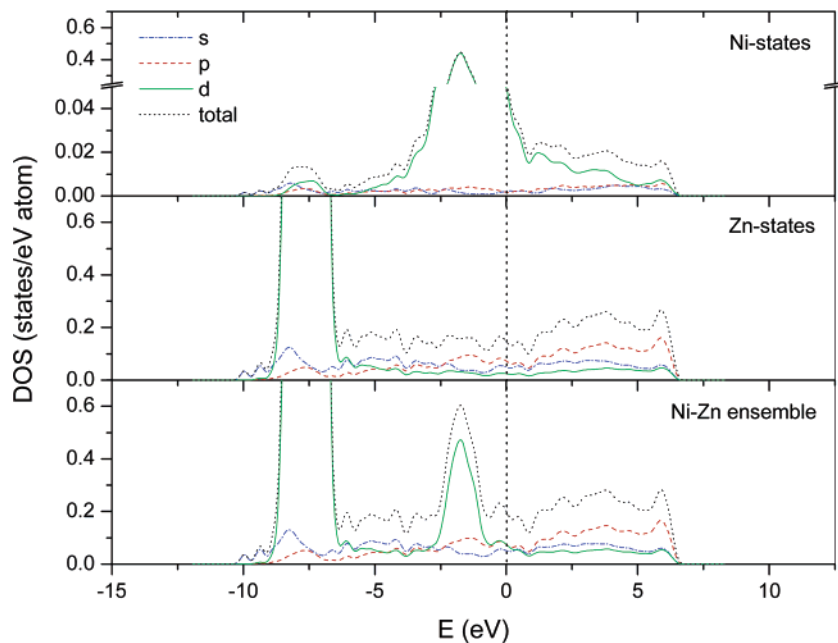


Figure 4. Total and partial density of states (DOS) of Ni-states, Zn-states, and Ni–Zn ensemble averaged over a few hundred configurations. The Fermi energy is shown as a dashed vertical line.

sponding to the MD cell. This is important in order to avoid the appearance of unphysical structures in the DOS.³⁷ The calculated electronic DOS for the three systems are presented in Figures 3, 4, and 5. The origin of the energy is taken to be the Fermi level. The states can be classified as *s*, *p*, and *d* states. The identification of these features is made straightforward by the examination of the partial DOS on the states, which are also shown in Figures 3, 4, and 5.

For the Ag–Zn ensemble, it is found that the DOS is finite at the Fermi energy, indicating that the alloy is metallic. The Fermi level falls into a deep minimum of

the DOS. We expect that there is a broad minimum in the electrical conductivity for the Ag–Zn ensemble. In Figure 3, we also decompose the DOS of Ag–Zn into contributions from Ag- and Zn-states. The Ag- and Zn-states stem from the Ag–Zn ensemble. Several characteristic features should be emphasized. (i) The DOS of the Ag-states is very small from -4 eV up to the Fermi level. Therefore the valence bands are dominated solely by the strong attractive potential of the Zn-states. In this sense, the Ag–Zn ensemble may be a charge-transfer compound. (ii) The Ag-states give rise to the low peak centered around -5 eV, while the high peak originates from the Zn-states. The low peak is superimposed by the Ag- and Zn-states from

(37) Genser, O.; Hafner, J. *Phys. Rev. B* **2001**, *63*, 144204.

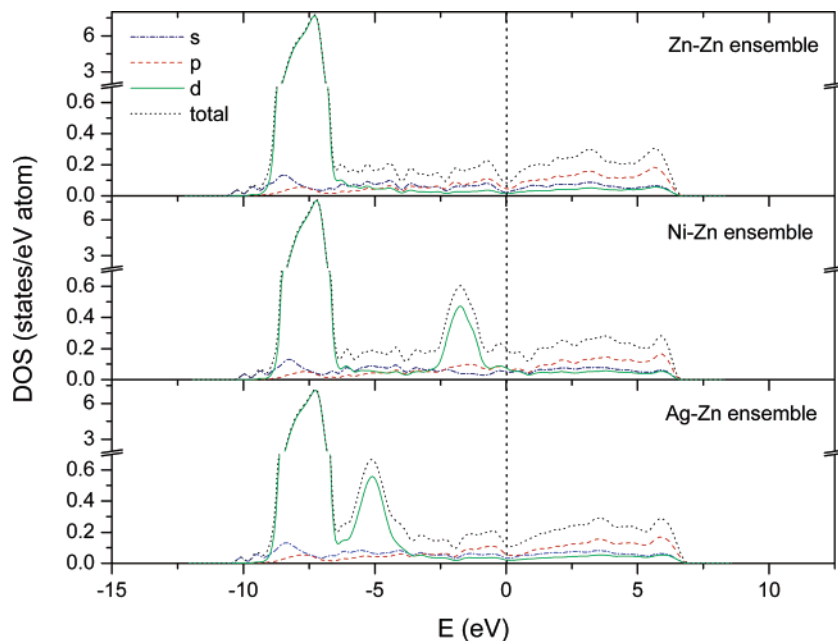


Figure 5. Total and partial density of states (DOS) of Ag–Zn, Ni–Zn, and Zn–Zn ensembles averaged over a few hundred configurations. The Fermi energy is shown as a dashed vertical line.

–6.2 eV to –3.7 eV. (iii) At the Ag-sites, the low-lying band at –7.6 eV has mixed *s*, *p*, *d*-character, yet the character of the band close to Fermi level is Ag-*d*. At the Zn-sites, the character of the band centered around –8 eV is Zn-*d*. This shows that the states mainly arise from the *d* bands. (iv) The strong resemblance of the DOS of the Ag–Zn ensemble with the Zn-states DOS indicates that the DOS of Ag–Zn is strongly dominated by Zn-states. (v) Above the Fermi level, the contribution of the Ag-states to the total DOS is very small. (vi) The Fermi level falls into a pseudogap separating the occupied Zn-states from the empty Ag-states. The presence of a pseudogap is energetically favorable for the electron transfer between the Zn- and Ag-states.

Although the DOS and partial DOS for the Ni–Zn ensemble are very similar to that found for the Ag–Zn ensemble, we note the differences between them. First, the large peak originating from the Ni-states is very close to the Fermi level. Thus, the valence bands arise from the Zn-states overlapping the Ni-states, indicating that the bands have mixed character. Second, the Fermi level does not fall into a pseudogap separating the occupied Zn-states from the empty Ni-states. This suggests that the electron transfer between the Zn- and Ni-states is energetically unfavorable.

In Figure 5, we compare the DOS and partial DOS for the Ag–Zn and Ni–Zn ensembles with that for the Zn–Zn ensemble. Even though the DOS for the three systems are quite similar, we observe some modifications as the additives Ag or Ni are added into Zn–Zn ensemble. First, the heights of the sharp peaks for the Ag–Zn and Ni–Zn ensembles slightly decrease compared with that of the Zn–Zn ensemble. Second, the Ag–Zn and Ni–Zn ensembles have somewhat narrower sharp peaks than the Zn–Zn ensemble. The changes are partly attributed to reduced band-filling due to slightly reduced Zn content in the molten alloy. However, one would expect that these reductions are over-compensated

by the smearing of the bands induced by the thermal disorder. Third, the DOS of the Ag–Zn and Ni–Zn ensembles present second peaks as the appearance of Ag or Ni in the Zn–Zn ensemble. The partial DOS reveal the nature of these changes. We note that the shape of the Zn partial DOS is essentially identical for Ag–Zn and Ni–Zn ensembles. The rigidity of the Zn partial DOS thus implies that the modifications in the DOS are mainly due to the changes in the partial DOS of Ag-states or Ni-states. Finally, the DOS at the Fermi level increase in the presence of Ag or Ni. The increases of the DOS at the Fermi energy are clearly due to the contributions from the Ag-states or Ni-states. All these changes are closely related to the modifications of the structures.

Finally, we turn to explaining the different results for the three ensembles on the basis of the electronic structure. From the above comparison of DOS, it is found that the valence bands of the Ni–Zn ensemble have mixed character of the Ni- and Zn-states, and yet that of Ag–Zn and Zn–Zn are dominated solely by the strong attractive potential of the Zn-states. The hybridization between the Ni- and Zn-states means that there are stronger interactions between atoms in the Ni–Zn ensemble than in the Ag–Zn and Zn–Zn ensembles. This suggests that the Ni–Zn ensemble has more nearest-neighbor atoms than Ag–Zn and Zn–Zn in the liquid. Thus, Ni–Zn has the highest coordination number among the ensembles. As the valence bands for Ag–Zn and Zn–Zn are very similar, the interactions between atoms for them are alike. Hence, they have nearly equivalent coordination numbers. These suggestions are supported by the calculated results displayed in Table 1. The Zn diffusion speed in the three ensembles also can be rationalized by applying the same elements. The stronger the interactions between atoms are, the slower the atom diffuses, and the smaller is its diffusion constant. Consider the Ni–Zn ensemble has stronger interactions between atoms than

the Ag–Zn and Zn–Zn ensembles, one may predict that diffusion constant of Zn atom for the Ni–Zn ensemble is smaller than that for the others. As we will show below, this is in complete agreement with our simulations.

3.4. Dynamic Properties. By following the atomic positions of the atoms in the liquid state as a function of time, we can calculate the diffusion constants of zinc in the Ag–Zn, Ni–Zn, and Zn–Zn ensembles. To obtain the true dynamics, we set the viscosity parameter to zero and followed the trajectory of each atom in the liquid state for 3 ps of the simulations. For sufficiently long time intervals, the diffusion constant can be obtained using the Einstein relation:

$$D = \lim_{t \rightarrow \infty} \frac{\langle [r(t)]^2 \rangle}{6t} \quad (1)$$

where $\langle [r(t)]^2 \rangle$ is the time-dependent mean-square displacement (averaged over all diffusing species) and t is the simulation elapsed time. This relation applies to periodic models only. The mean-square displacement of a species j at any time step n , $r_{n,j}^2$ is calculated as the time-average³⁸

$$\overline{r_{n,j}^2} = \frac{1}{n} \sum_{i=1}^n [r_i(t) - r_i(0)]^2 \quad (2)$$

where $r_i(t)$ is the position of the diffusing species' center of mass at time step i . The initial time may be set arbitrarily, provided the simulation is run sufficiently long. In our calculations, we computed the average taking the beginning of each time step as a different time origin. Then $\langle [r(t)]^2 \rangle$ is related to $\overline{r_{n,j}^2}$ as

$$\langle [r(t)]^2 \rangle = \frac{1}{m} \sum_{j=1}^m \overline{r_{n,j}^2} \quad (3)$$

where m is the total number of diffusing species of type j .

Figure 6 presents plots of the mean-square atomic displacement as a function of time for Ag–Zn, Ni–Zn, and Zn–Zn ensembles at a temperature of 723 K. The ideal asymptotic form shown in eq 1 assumes perfect averaging over a simulation of infinite duration. Actually, the asymptotic linear behavior of mean-square atomic displacement is attained after only a few tenths of a ps in all normal liquids. It may be seen from Figure 6 that our curves show this asymptotic linear behavior. The lack of straightness of the curves at long times is simply an effect of statistical averaging. Fitting these curves by linear time dependence (last 2.5 ps) produces the diffusion constant. The calculated zinc diffusion constants are listed in Table 2 along with the experimental result.³⁹

For the Zn–Zn ensemble, we obtain a self-diffusion constant of $2.48 \times 10^{-9} \text{ m}^2/\text{s}$, very close to the experimental value of $2.37 \times 10^{-9} \text{ m}^2/\text{s}$ for pure liquid zinc.³⁹ It is found from Table 2 that the Zn diffusion constants

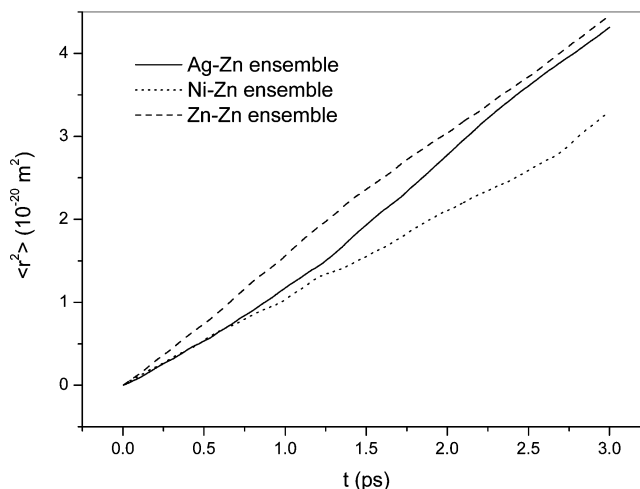


Figure 6. Calculated mean-square atomic displacements $\langle r^2 \rangle$ of zinc atom versus time t for Ag–Zn, Ni–Zn, and Zn–Zn ensembles at 723 K.

Table 2. Calculated and Measured Zinc Diffusion Constants D ($10^{-9} \text{ m}^2/\text{s}$) for Ag–Zn, Ni–Zn, and Zn–Zn Ensembles at 723 K

	Ag–Zn	Ni–Zn	Zn–Zn
this work	2.51	1.75	2.48
experiment ^a			2.37

^a Ref 39.

of different ensembles increase in the following order: Ag–Zn \approx Zn–Zn $>$ Ni–Zn. This shows that the Zn diffusion speed in different ensembles varies in the following sequence: Ag–Zn \approx Zn–Zn $>$ Ni–Zn. This trend is in agreement with the additive effects on the thickness of coatings in galvanizing, where Ag increases the coating thickness, but Ni decreases it.

For Ag–Zn, Ni–Zn, and Zn–Zn ensembles, our calculated results are supported by the observed additive effects in steel hot-dip galvanizing. Our MD simulations reveal that the role of additives in controlling the zinc coating thickness is to alter zinc diffusion speed before reaching the substrate. These suggestions may be useful for screening chemical additives to control the zinc coating thickness.

4. Conclusions

In this study, we have performed ab initio MD simulations to study the effects of additives Ag and Ni on Zn diffusion in steel hot-dip galvanizing. Ag–Zn, Ni–Zn, and Zn–Zn ensembles are selected to model the industry process. We examine differences in the structural and electronic properties among the Ag–Zn, Ni–Zn, and Zn–Zn associates. Diffusion constants of Zn atoms for the dynamic properties of these associates are presented.

For the Zn–Zn ensemble, the calculated pair correlation function, first peak position, and coordination number are in good agreement with available experimental data. It is found that additions of Ag or Ni do not change the positions of the peaks in the pair correlation function, which remain almost the same as those found for pure liquid zinc, but they alter the maxima and minima of the peaks. The coordination numbers of different ensembles increase in the following order: Ni–Zn $>$ Ag–Zn \approx Zn–Zn.

(38) Allen, M. P.; Tildesley, D. J. *Computer Simulation of Liquids*; Clarendon Press: Oxford, 1987.

(39) Nachtrieb, N. H.; Fraga, E.; Wahl, C. *J. Phys. Chem.* **1963**, *67*, 2353.

The DOS for the three systems are similar, but some modifications are observed as the additives Ag or Ni are added into Zn–Zn ensemble. These changes are closely related to the modifications of the structures.

For the Zn–Zn ensemble, the Zn self-diffusion constant is calculated to be 2.48×10^{-9} m²/s, very close to the experimental value of 2.37×10^{-9} m²/s. The Zn diffusion constants of different ensembles increase in the following order: Ag–Zn \approx Zn–Zn > Ni–Zn. This

trend is in agreement with the additive effects on the thickness of coatings in galvanizing, where Ag increases the coating thickness, but Ni decreases it.

Our MD simulations reveal that the role of additives in controlling the zinc coating is to alter the zinc diffusion speed before reaching the substrate. These suggestions may be useful for screening chemical additives to control the zinc coating thickness.

CM0488635